Chapter 2
Identification of Species by Electrochemical Methods

2.1 Introduction

As previously noted, the identification of components in works of art and archaeological objects is a difficult task during their scientific examination. Samples usually appear as heterogeneous or (apparently) homogeneous solid materials, frequently incorporating different portions; for instance, preparative, pigmenting, and protective layers in paints. At first glance, conventional electrochemical methods are applicable for identifying pigmenting species in solutions resulting from the chemical attack of acids, bases, and organic solvents, etc., of the solid sample. This approach offers two main drawbacks: (i) the disposal of sample amounts restricted to the ng-μm range, thus requiring high sensitive methods, and especially (ii) the loss of analytical information due to the chemical attack on the sample. Thus, an acidic attack of a sample containing either red or yellow cadmium pigments yields Cd^{2+} ions in solution, which can be identified by conventional stripping voltammetry. However, this procedure does not inform on the composition of the original pigment.

Solid state voltammetric methods can be used to obtain information on the composition of the materials used in works of art. Here, the methodology of the voltammetry of microparticles, developed by Scholz et al. [72, 73], will be presented. This methodology provides qualitative, quantitative, and structural information on sparingly soluble solid materials, as described in extensive reviews [74–77] and a precedent monograph [78], just requiring sample amounts in the ng-μg level.

2.2 Conventional Voltammetry

Although a variety of electrochemical methods are available, voltammetry (based on the record of the current i flowing across an electrochemical cell under the application of a given time-depending potential E) has become the most important measuring technique in pure and applied electrochemistry [79].

Generally, a voltage is applied between a working electrode and an auxiliary electrode, and the potential of the working electrode is controlled versus the reference electrode possessing a constant and known potential. The current flowing through

A. Doménech-Carbó et al., *Electrochemical Methods in Archaeometry, Conservation and Restoration*, Monographs in Electrochemistry,
DOI 10.1007/978-3-540-92868-3_2,

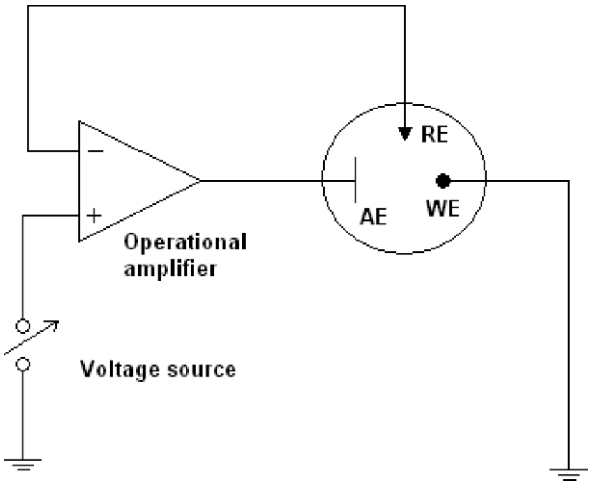

Fig. 2.1 Scheme for a conventional three-electrode voltammetric cell. RE = reference electrode; WE = working electrode; and AE = auxiliary electrode

the working and auxiliary electrodes is the response to the potential of the working electrode—i.e., the excitation signal. Usually a three-electrode arrangement is used, as schematized in Fig. 2.1. In this equipment, a potentiostat controls the potential so that the current flows almost exclusively between the working electrode and the auxiliary electrode, while a very small, practically negligible current is passing through the reference electrode—usually AgCl/Ag, or Hg_2Cl_2/Hg (calomel) electrodes.

Depending on the time variation of the applied potential, several types of voltammetry can be distinguished. Among them, the most widely used are linear and cyclic voltammetries. Here, the excitation signal is a linear potential scan that is swept between two extreme values, and in cyclic voltammetry the potential is swept up and down between the two values (or switching potentials) with the same absolute scan rate (v, usually expressed in mV/s), although it has the opposite sign [79].

In conventional cyclic and linear sweep voltammetry, electrochemical measurements are performed in a quiescent solution of an electroactive species contained in a given electrolyte. The concentration of the electroactive species is typically between 10 µM and 1 mM, while a supporting electrolyte—typically in 0.10 M concentration—is added. The resulting solution must generally be deoxygenated to avoid perturbing signals and possible secondary reactions with dissolved oxygen. Purging the solution with nitrogen or argon for 5–15 min is performed for this purpose.

Figure 2.2 shows the first-scan cyclic voltammogram obtained by a platinum electrode for a 1.0 mM $K_4[Fe(CN)_6]$ plus 0.10 M KCl solution in water. Here, as in all figures in this chapter, potentials are referred to the AgCl (3 M NaCl)/Ag electrode. Generally, the first recorded cycles differ slightly, and only after 3–4 cycles do the CVs approach a constant response. In this experiment, the potential scan is

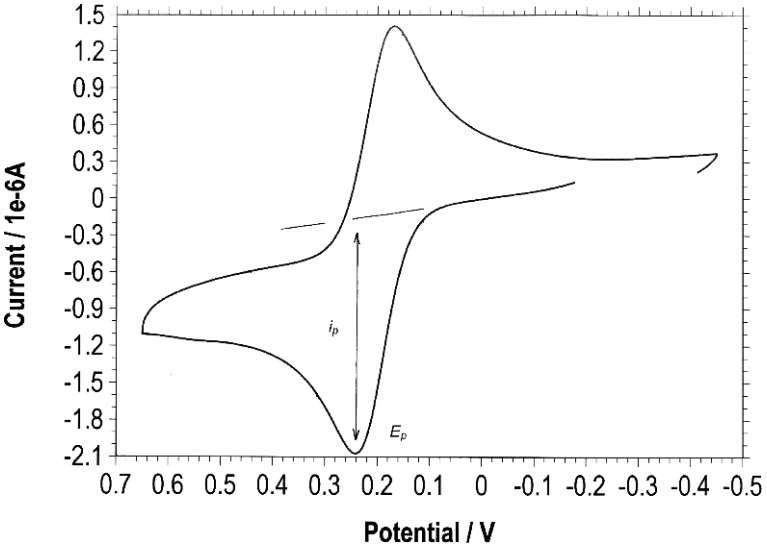

Fig. 2.2 Cyclic voltammogram at Pt electrode for a 1.0 mM $K_4Fe(CN)_6$, plus 0.10 M KCl solution. Potential scan rate of 50 mV/s. The peak current measured from the base line and the peak current for the anodic peak are marked

initiated at -0.18 V in the positive direction, and switches at $+0.65$ V, thus defining an initial anodic (oxidative) scan. In the subsequent scan, the potential is negatively shifted, defining a cathodic (reductive) scan until the new switching potential of -0.45 V is reached. In this system, a redox process based on the oxidation of iron ions in their oxidation state $+2$ to iron ions in a $+3$ oxidation state can occur. This defines a $[Fe(CN)_6]^{3-}/[Fe(CN)_6]^{4-}$ redox couple, characterized by a mid-peak potential E_{mp} that can, under certain conditions, be taken as a good approximation for the formal electrode potential $E_c^{\circ\prime}$ of the redox system—in turn, directly related to the thermodynamic electrode potential E°.

Initially, at potentials between -0.25 and about $+0.1$ V, a rather low current is recorded due to double-layer charging. Later, when the potential is sufficiently positive to oxidized $[Fe(CN)_6]^{4-}$ to $[Fe(CN)_6]^{3-}$, the anodic current increases rapidly until the concentration of $[Fe(CN)_6]^{4-}$ at the electrode surface is substantially diminished. Then, the (anodic) current increases dramatically until a maximum value is reached, thus defining a (anodic) voltammetric peak with the peak potential E_{pa} and the peak current i_{pa}. The correct peak current must be measured in relation to the background current, which can be extrapolated from the starting region. After the peak, the current decreases slowly as the electrode is depleted of $[Fe(CN)_6]^{4-}$ due to its electrochemical conversion into $[Fe(CN)_6]^{3-}$. When the (anodic) switching potential $E_{\lambda a}$ is attained, the potential scan reverses its direction. In the subsequent cathodic scan, a similar cathodic peak is measured, defining a cathodic peak potential E_{pc} and a cathodic peak current i_{pc}. Then, the current reaches a maximum and subsequently decays.

This system can be taken as an example of so-called reversible, diffusion-controlled electrochemical processes. In short, during the initial anodic scan, an electron-transfer process between the ferrocyanide (or hexacyanoferrate(II)) ions, $[Fe(CN)_6]^{4-}$, and the working electrode occurs. This can be represented by means of the equation (here, aq denotes species in aqueous solution):

$$[Fe(CN)_6]^{4-}_{aq} \rightarrow [Fe(CN)_6]^{3-}_{aq} + e^- \tag{2.1}$$

This process can be described in terms of a heterogeneous reaction in which ferricyanide (or hexacyanoferrate(III)) ions, $[Fe(CN)_6]^{3-}$, are formed. At the beginning of the voltammetric peak, the current is controlled by the kinetic of the electron transfer across the electrode/electrolyte barrier so that the current increases somewhat exponentially with the applied potential. The value of the current is controlled 150–200 mV after the voltammetric peak by the diffusion rate of ferrocyanide ions from the solution bulk toward the electrode surface.

In the reverse (cathodic) scan, ferricyanide ions remaining in the vicinity of the electrode surface are reduced to ferrocyanide ones. This process can be represented by the inverse of Eq. 2.1, with the voltammetric profile being interpreted from considerations similar to those made for the anodic peak.

The theory for cyclic voltammetry was developed by Nicholson and Shain [80]. The mid-peak potential of the anodic and cathodic peak potentials obtained under our experimental conditions defines an electrolyte-dependent formal electrode potential for the $[Fe(CN)_6]^{3-}/[Fe(CN)_6]^{4-}$ couple $E^{\circ\prime}$, whose meaning is close to the genuine thermodynamic, electrolyte-independent, electrode potential E° [79, 80]. For electrochemically reversible systems, the value of $E^{\circ\prime}$ $(= (E_{pc} + E_{pa})/2)$ remains constant upon varying the potential scan rate, while the peak potential separation provides information on the number of electrons involved in the electrochemical process: $(E_{pa} - E_{pc}) = 59/n$ mV at 298 K [79, 80]. Another interesting relationship is provided by the variation of peak current on the potential scan rate: for diffusion-controlled processes, i_p becomes proportional to the square root of the potential scan rate, while in the case of reactants confined to the electrode surface, i_p is proportional to v [79].

In voltammetric experiments, electroactive species in solution are transported to the surface of the electrodes where they undergo charge transfer processes. In the most simple of cases, electron-transfer processes behave reversibly, and diffusion in solution acts as a rate-determining step. However, in most cases, the voltammetric pattern becomes more complicated. The main reasons for causing deviations from reversible behavior include: (i) a slow kinetics of interfacial electron transfer, (ii) the presence of parallel chemical reactions in the solution phase, (iii) and the occurrence of surface effects such as gas evolution and/or adsorption/desorption and/or formation/dissolution of solid deposits. Further, voltammetric curves can be distorted by uncompensated ohmic drops and capacitive effects in the cell [81–83].

Corresponding to a cyclic voltammogram (CV), recorded at a glassy carbon electrode (GCE) immersed into a 1.0 mM Cu^{2+} solution in acetic acid/sodium acetate

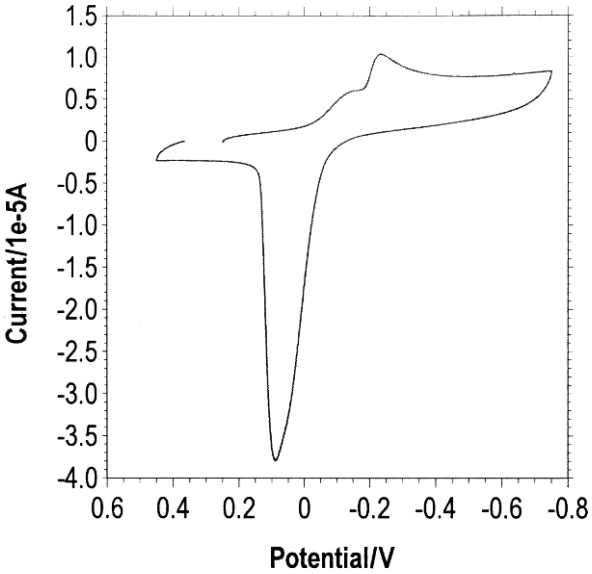

Fig. 2.3 Cyclic voltammogram at GCE for a 1.0 mM solution of $CuSO_4 \cdot 5H_2O$ in 0.25 M HAc + 0.25 M NaAc, pH 4.85. Potential scan rate 50 mV/s

buffer, Fig. 2.3 allows for an examination of some of these processes. Here, the potential is initially scanned in a negative direction so that a main reduction peak appears at -0.22 V. In the subsequent anodic scan, a sharp oxidation peak is recorded at $+0.08$ V. The initial two-electron reduction of copper ions can be represented as:

$$Cu^{2+}{}_{aq} + 2e^- \rightarrow Cu_s \tag{2.2}$$

As a result of that reductive process, a deposit of copper metal (denoted in Eq. 2.2 by "s" for "solid") is formed on the carbon electrode surface. The prominent anodic peak recorded in the reverse scan corresponds to the oxidative dissolution of the deposit of copper metal previously formed. The reason for the very intense anodic peak current is that the copper deposit is dissolved in a very small time range (i.e., potential range) because, in the dissolution of the thin copper layer, practically no diffusion limitations are involved, whereas in the deposition process (i.e., the cathodic peak), the copper ions have to diffuse through the expanding diffusion layer from the solution to the electrode surface. These processes, labeled as stripping processes, are typical of electrochemically deposited metals such as cadmium, copper, lead, mercury, zinc, etc., and are used for trace analysis in solution [84]. Remarkably, the peak profile is rather symmetrical because no solution-like diffusive behavior is observed.

For analytical purposes, voltammetric peaks can be used for identifying species in a solution phase, provided that a well-defined electrochemical response is obtained. Application of that methodology implies a sample treatment is needed to

dissolve electroactive components. Examples involve extraction of organic dyes in fibers and inks by organic solvents or attack of metallic fragments by mineral acids.

The use of analytical procedures based on conventional voltammetry requires the selection of a solvent, a supporting electrolyte, an electrode, an electrochemical technique, electrochemical parameters, and data treatment:

(a) Solvent selection derives from a compromise between the desired solubility of the analyte(s) and the available potential range. The solvent, electrolyte, and electrode material determine the potential window of operative potentials. Thus, in neutral aqueous solutions with graphite electrodes, large cathodic currents appear due to water reduction into hydrogen at about -1.25 V vs. saturated calomel electrode (SCE), while large anodic currents are recorded above $+1.25$ V due to water oxidation into oxygen. With gold and platinum electrodes, hydrogen discharge is favored, and the available potential range is restricted to the potential region between -1.00 and $+1.25$ V.

(b) In organic solvents such as CH_3CN (MeCN), $(CH_3)_2SO$ (DMSO), HCON $(CH_3)_2$ (DMF) or CH_2Cl_2, the salts Et_4NClO_4 and Bu_4NPF_6 (among others) are the most used supporting electrolytes. In aqueous solutions, a variety of supporting electrolytes can be used, from salts ($NaCl, NaClO_4$) to acids (HCl, H_2SO_4, HNO_3) to alkalis (NaOH,KOH). The use of buffers such as acetate and phosphate in concentrations of 0.10–0.50 M allows for reproducible experimental conditions. In some instances, complexing agents such as EDTA, oxalate, and tartrate can be added.

(c) The electrode material can seriously condition the observed response, as previously noted. Apart from solvent discharge effects, electrodes are to always "active" to some extent. Thus, in contact with aqueous electrolytes, mercury electrodes are oxidized to Hg_2^{2+} and Hg^{2+} at potentials above $+0.20$ V vs. AgCl/Ag, while gold and platinum electrodes form surface oxides at potentials ca. $+1.0$ V.

(d) Linear potential scan and cyclic voltammetries (LSV and CV, respectively) are the most widely used electrochemical techniques. Of course, nonvoltammetric techniques, such as controlled potential and controlled current coulometry, chronoamperometry, and chronopotentiometry, can also be used. Within the context of voltammetric methods, other techniques are available using a suitable function generator. In differential pulse voltammetry (DPV), potential pulses are superimposed to a linear potential scan [79]. In square wave voltammetry (SQWV), a square wave signal comprised of the sum of a symmetrical square wave of half peak-to-peak amplitude E_{SW} and a staircase of the same period τ is used. The potential increment of the staircase is ΔE. The current is sampled at the end of each pulse to yield forward and reverse currents. Their difference is the net current. These above techniques minimize capacitive effects and yields tall peaks, thus facilitating resolution in systems displaying multiple signals [85].

(e) Electrochemical parameters can be varied within relatively large intervals, thus modulating the observed electrochemical response. In cyclic voltammetry, increasing potential scan rate generally results in increasing peak currents, but in a concomitant increase of background currents (and shape-distorting capacitive

and resistive effects, in particular), as well as in a decrease of peak resolution. In pulse techniques, pulse amplitude, pulse width, and pulse intervals can be varied, resulting in different conditions for studying electrochemical processes. Variation of such parameters allows performance of voltammetric experiments in "short-time" and "long-time" experiments with experimentation times between 0.1–1 ms and 10–100 min, respectively.

(f) Current electrochemical equipment routinely provides computer-assisted treatment of data, determining peak current and peak potential, peak area, and displaying derivative and integral curves. Derivative and integral techniques can be used for improving peak resolution. In particular, semiderivation (deconvolution) and semi-integration (convolution) techniques are frequently used [86].

This is illustrated in Fig. 2.4, where the deconvolution of differential pulse voltammograms at the glassy carbon electrode in the ethanol extract from two commercial inks are shown. Samples were taken from paper fragments of 0.10 mg immersed for 10 min in a 50:50 (v/v) ethanol: 0.50 M aqueous acetate buffer (pH 4.85) solution.

Since low volumes of solution and low analyte concentrations are involved in samples from works of art and archaeological pieces, low-volume cells (1–2 mL) can also be used coupled with micro- and ultramicroelectrodes. These last provide high sensitivity and allow operation with electrolytes of low dielectric constant or even work without supporting electrolytes [87, 88].

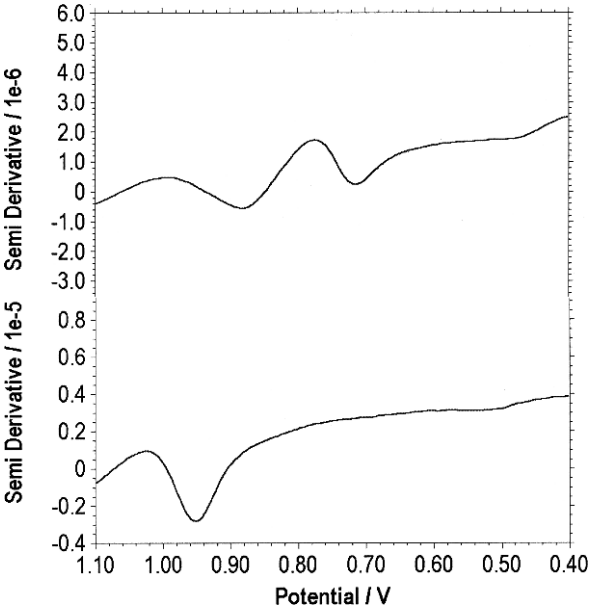

Fig. 2.4 Deconvolution of differential pulse voltammograms at the glassy carbon electrode in the ethanol extract from two commercial inks transferred to a 50:50 (v/v) ethanol:0.50 M aqueous acetate buffer (pH 4.85) solutions. Voltammograms for red (upper) and blue (below) commerical inks

2.3 Voltammetry of Microparticles

The application of solution phase electrochemistry for studying the work of art samples and archaeological artifacts requires, as previously indicated, sample treatment via extraction or chemical attack. This is an obvious drawback, because these operations, apart from the requirement of relatively high amounts of sample, usually lead to a loss of information since the solid is dissolved and all signals that are specific for the solid compound or material are not available anymore for measurements.

The first use of electrochemical methods for identifying components in solid samples can be attributed to Fritz [89] and Glazunov [90], who developed the electrography. Here, two inert electrodes are connected to a potential source, and one is brought into contact with the solid sample (mineral fragment, coin, metallic artifact), which is placed with one rim in contact with a filter paper moistened with a selected electrolyte. The second electrode is connected with the filter paper. In the most common version, the current is allowed to pass for a few seconds so that metallic constituents experience an anodic dissolution. A related procedure was the Weisz ring-oven method [91], further developed by Stephen [92], with direct application to the analysis of coins. Identification and semiquantitation of metal ions can be performed colorimetrically by adding the adequate reactants to the electrolyte, which impregnates the filter paper (diethyldithiocarbamate, demiethylglyoxime, $K_4Fe(CN)_6$, etc.). As a result, both qualitative [93–95] and semiquantitative [96] analysis of metal cations from the solid sample have been reported.

Carbon paste electrodes (CPEs), introduced in the 1960s by Kuwana et al. [97, 98], and further studied by Bauer et al. [99–101] and Brainina et al. [102, 103], were the most widely used approach for studying the electrochemical response of solids. Here, the solid is dispersed into a conducting paste formed by graphite powder and an organic (nujol oil, paraffin oil, etc.) or inorganic (aqueous electrolytes, such as H_2SO_4) binder. Although CPEs have produced a relatively extensive literature focused on mineral analysis using both organic [104] and inorganic [105] binders, their application to pigment analysis suffers from the presence of large background currents and the high sensitivity of the electrochemical response to changes in the composition of the binder. In 1989, Scholz et al. [72, 73] introduced the voltammetry of microparticles (also called abrasive stripping voltammetry, when the transferred solid is electrochemically dissolved during the measurement), where the solid sample is transferred by abrasion to the surface of paraffin-impregnated graphite electrodes (PIGEs). This methodology provides large signal-to-background responses and excellent repeatability, allowing for identification of inorganic [106] and organic [107] pigments. Alternative approaches involve graphite-polymer composites [108], formation of fine deposits of the solid sample by evaporation of solutions [109] or suspensions [110] of the solid on conventional electrodes, and attachment of solid microparticles to polymer coatings (polymer film electrodes, PFEs) [111, 112]. Selection of the type of electrode modification may be crucial for obtaining an electrochemical response that is useful for analytical purposes.

Thus, the study of the electrochemistry of nonconducting solid materials requires their "contact" with a substrate electrode or their dispersion into a conducting matrix. In typical carbon paste electrodes, a small amount of the solid analyte is mixed with graphite powder plus a nonelectrolyte binder to form a conducting past [97, 98, 104]. Then, the electron transfer processes occur at the paste-electrolyte interface, the currents are smaller, and the surface coverage can be minimized. However, the particle size distribution, the nature of the binder, and paste composition influence the electrochemical response, which frequently exhibits poor reproducibility. These problems can be solved in part by using an electrolyte binder that ensures large conductivity within the paste [99–101, 105, 113, 114]. However, aggressive binders may dissolve the solid analyte or produce undesirable chemical reactions.

These drawbacks can be avoided to a large extent, using the voltammetry of microparticles—a technique involving solid state electrochemistry where down to about 10^{-6} to 10^{-11} mol of sample [74–78] can be transferred by abrasion into the surface of an inert electrode, usually paraffin-impregnated graphite electrodes, and the electrode is later immersed in a suitable electrolyte for recording its voltammetric response. The response of this sample-modified electrode, consisting of the reduction or oxidation of the solid materials, becomes phase-characteristic.

As in solution phase electrochemistry, selection of solvent and supporting electrolytes, electrode material, and method of electrode modification, electrochemical technique, parameters and data treatment, is required. In general, long-time voltammetric experiments will be preferred because solid state electrochemical processes involve diffusion and surface reactions whose typical rates are lower than those involved in solution phase electrochemistry.

A paradigmatic example is provided by an extensively used pigment: Prussian blue— potassium-iron(III) hexacyanoferrate(II), also called potassium-iron(III) ferrocyanide. This is constituted by potassium-iron(III) ferrocyanide, $KFe[Fe(CN)_6]$, whose electrochemistry has been extensively studied [74–77].

As shown in Fig. 2.5, the cyclic voltammograms for Prussian blue attached to paraffin-impregnated graphite electrodes (PIGEs) in contact with aqueous electrolytes exhibit two well-defined one-electron couples. Prussian blue crystals possess a cubic structure, with carbon-coordinated Fe^{2+} ions and nitrogen-coordinated Fe^{3+} ions, in which potassium ions, and eventually some Fe^{3+} ions, are placed in the holes of the cubes as interstitial ions. The redox couple at more positive potentials can be described as a solid-state process involving the oxidation of Fe^{2+} ions. Charge conservation requires the parallel expulsion of K^+ ions [77]:

$$KFe^{III}[Fe^{II}(CN)_6]_s \rightarrow Fe^{III}[Fe^{III}(CN)_6]_s + K^+{}_{aq} + e^- \tag{2.3}$$

The process at more negative potentials must correspond to the reduction of Fe^{3+} ions coupled with the insertion of K^+ ions from the electrolyte:

$$KFe^{III}[Fe^{II}(CN)_6]_s + K^+_{aq} + e^- \rightarrow K_2Fe^{II}[Fe^{II}(CN)_6]_s \tag{2.4}$$

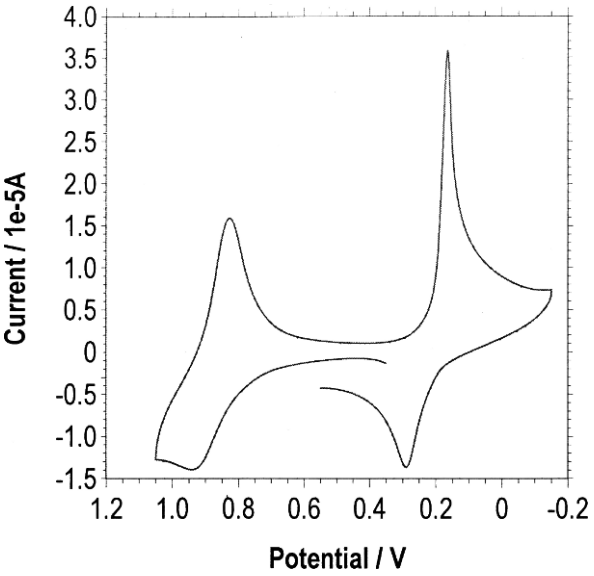

Fig. 2.5 Cyclic voltammogram for a Prussian-blue modified PIGE immersed in 0.10 M KCl. Potential scan rate 10 mV/s

Such electrochemical processes can be described on the basis of the model developed by Lovric and Scholz [115, 116] and Oldham [117] for the redox reactivity of nonconducting solids able to be permeated by cations or anions (so-called ion-insertion solids). As described in the most recent version of Schröder et al. [118], the electrochemical process is initiated at the three-phase junction between the electrode, the electrolyte solution, and the solid particle, as schematized in Fig. 2.6. From this point, the reaction expands via charge diffusion across the solid particle. It is assumed that, for a reduction process, there is a flux of electrons through the

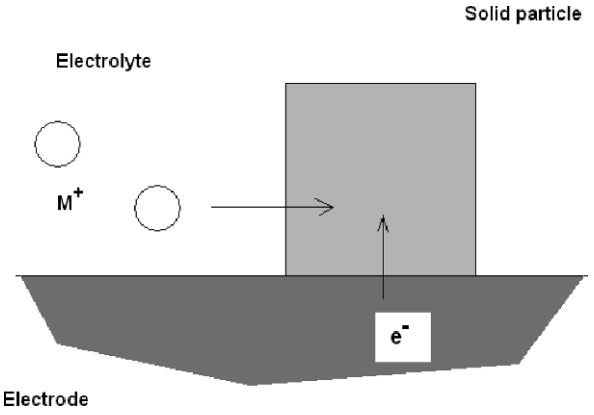

Fig. 2.6 Schematic diagram for describing electrochemical processes (reduction) on a nonconducting solid, allowing for both electron and ion transport

electrode/particle interface, coupled with a flux of electrolyte ions across the electrolyte/particle interface. The electrochemical reaction progresses via electron hopping between immobile redox centers in the solid, accompanied by the migration of charge-balancing electrolyte cations through the solid (electron diffusion and cation diffusion, respectively). A pictorial representation of the described mechanism is illustrated in Fig. 2.6. Obviously, an equivalent description is eventually obtained if the insertion of cations into the solid is replaced by the issue of mobile anions from the solid to the electrolyte.

The relevant point to emphasize is that this model allows one to justify the existence of solid-state electrochemical reactions. Remarkably, the redox conductivity is maintained even in the limiting cases where electron diffusion or cation diffusion are hindered. Here, the electrochemical reaction may progress via surface diffusion along the external layer of the particle in contact, respectively, with the electrode and the electrolyte.

The foregoing considerations can also be applied to the electrochemistry of a number of organic compounds in contact with aqueous buffers [107, 119–125]. Here, protonation/deprotonation reactions are coupled with electron transfer processes, as described for the case of indigoid-, anthraquinonic-, and flavonoid-type pigments, among others. In contact with aqueous electrolytes, the electrochemical processes can generally be described as:

$$A^{ox}{}_s + qH^+{}_{aq} + qe^- \rightarrow H_qA^{rd}{}_s \tag{2.5}$$

where A^{ox} represents the oxidated form of the organic species and H_qA^{rd} represents the q-protonated reduced form. Figure 2.7 shows a pictorial representation of such electrochemical processes.

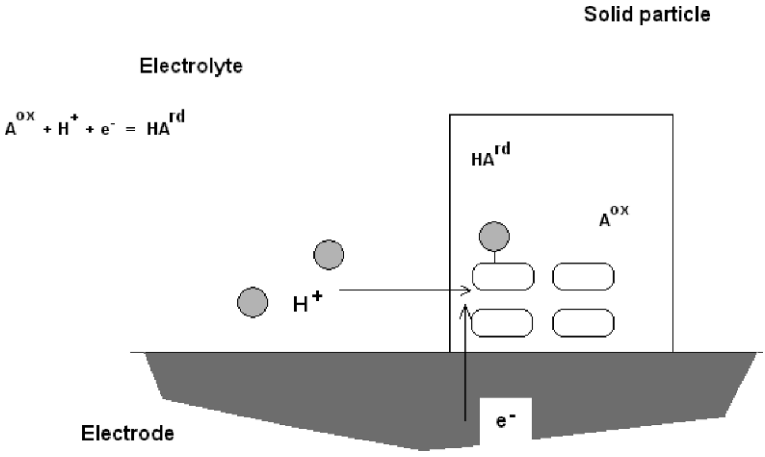

Fig. 2.7 Schematic representation of electrochemical processes (reduction) for organic solids able to experience coupled proton transport/electron transport processes

2.4 Identification of Species Involving Electrochemically Depositable Metals

An important class of solid state electrochemical reactions involves the reduction of metal oxides or salts to the corresponding metals. This situation applies for cadmium, cobalt, copper, lead, mercury, and zinc pigments, whose electrochemical identification using the voltammetry of microparticles approach has recently been discussed for pictorial samples [108, 111, 126, 127] and ceramic pigmenting species [112, 128, 129]. In Fig. 2.8, the cyclic voltammogram is obtained from a $PbCO_3$-modified PIGE immersed into an acetate buffer. This response can be described in the following terms. In the initial cathodic scan, $PbCO_3$ is reduced at -0.60 V to lead metal, the overall process being

$$PbCO_{3s} + 2H^{+}_{aq} + 2e^{-} \rightarrow Pb_s + CO_2 + H_2O \tag{2.6}$$

As before, the subscript s denotes solid phases, and the subscript aq denotes solvated ions in solution. As a result of this process, a deposit of lead metal is formed on the electrode surface at the end of the cathodic scan while CO_2 diffuses to the

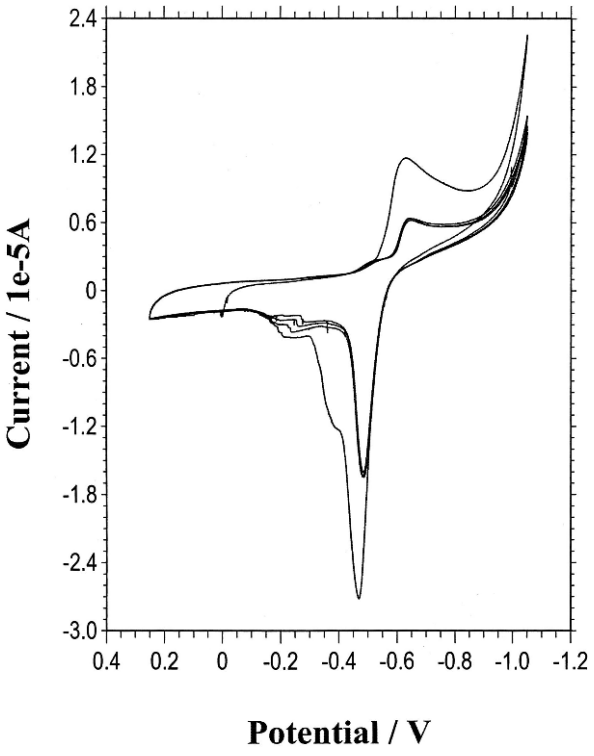

Fig. 2.8 Cyclic voltammogram for a $PbCO_3$-modified PIGE immersed into 0.50 M sodium acetate buffer at pH 4.85. Potential scan rate 50 mV/s

solution bulk. In the subsequent anodic scan, the metallic lead is oxidized to Pb^{2+} ions in solution via an oxidative dissolution process labeled as "oxidative stripping" at −0.48 V:

$$Pb_s \rightarrow Pb^{2+}{}_{aq} + 2e^- \tag{2.7}$$

Sharp stripping peaks produce large peak currents. In fact, stripping peaks are systematically used in trace analysis for metal ion determination in solution [84].

Upon repetitive cycling of the potential scan, the voltammetric record is reproduced, but an additional cathodic peak near to −0.45 V appears. This is due to the reduction of Pb^{2+} ions electrochemically generated by the previous oxidation of lead metal. The reduction of lead ions occurs at a potential different from that at which the reduction of $PbCO_3$ takes place. In repetitive voltammetry, additional anodic peaks appear at −0.40 and −0.28 V. These are due to the oxidative dissolution of different lead deposits generated in reductive scans [130, 131].

Formation of lead deposits can be monitored by coupling atomic force microscopy (AFM) with electrochemical experiments. Figure 2.9 shows AFM images recorded for Naples yellow (lead antimoniate, $Pb(AsO_3)_2$) deposited onto a carbon plate in contact with acetate buffer. Here, deposits of lead metal appear as sharp grains in the vicinity of the aggregates of the pigment. This situation is similar to that described for litharge (yellow form of PbO) by Scholz et al. [130, 132]. Here, in situ

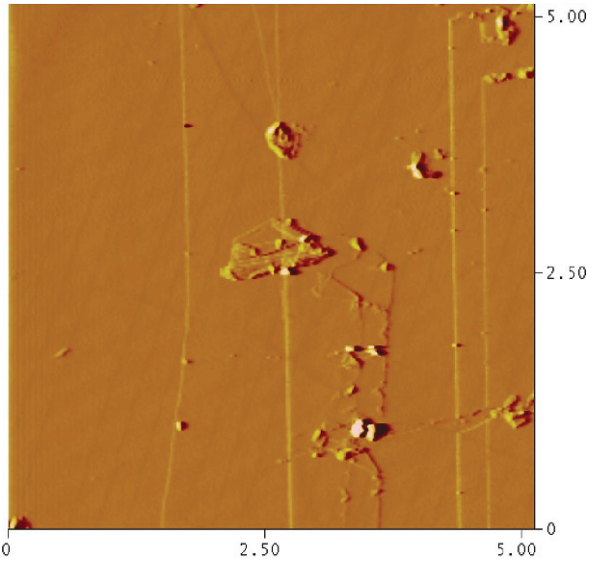

Fig. 2.9 AFM image of a deposit of Naples yellow on a carbon plate in contact with 0.20 M HAc + 0.25 M NaAc at pH 4.85, after application of a potential step of −0.75 V over 2 min [126]

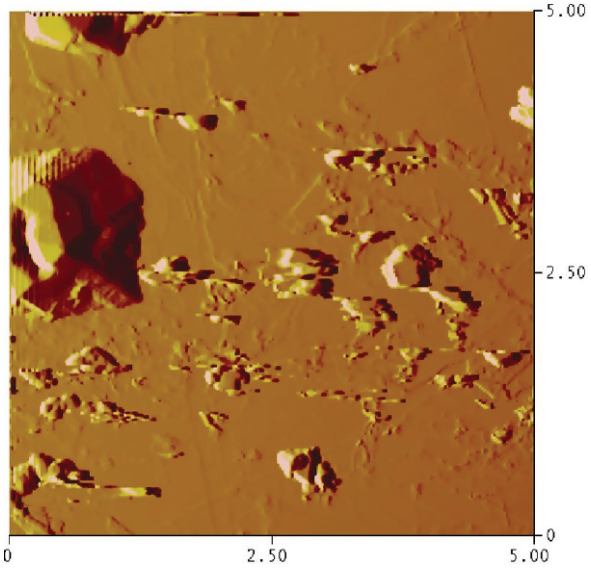

Fig. 2.10 AFM image of a deposit of minium on a carbon plate in contact with 0.20 M HAc + 0.25 M NaAc at pH 4.85, after application of a potential step of −0.75 V over 2 min [126]

XRD [132] and AFM [130] data suggests that the electrochemical mechanism involves a solid state epitactic transformation of lead oxide to lead metal.

In some cases, the deposit of lead metal also consist of irregular aggregates far from the original particles of the lead compound [126], as can be seen in Fig. 2.10 for minium (Pb_3O_4)—another widely used pigment These features can be rationalized, assuming that the electrochemical pathway represented by Eq. 2.6 can eventually be coupled by a reductive process via formation of Pb^{2+} in solution

$$PbO_s + 2H^+{}_{aq} + 2xe^- \rightarrow (1-x)Pb^{2+}{}_{aq} \cdots + xPb_s + H_2O \qquad (2.8)$$

further reduced to lead metal via the process inverse to that described by Eq. 2.7.

For our purposes, the relevant point to emphasize is that the different lead pigments yield different reductive responses [126]. Detailed electrochemical analysis indicated that, for a given electrolyte and material, the peak potential and the morphology of the cathodic signals depend slightly on the shape and size distribution of solid particles [73–78].

The shape and position of the anodic stripping peak should be, in principle, independent of the starting material. This peak, however, is influenced by the conditions of metal deposition. Thus, as described by Komorsky-Lovric et al. [131], the stripping peak of electrochemically deposited lead differs from that recorded for lead compounds mechanically attached to graphite electrodes. Additionally, the presence of other depositable metals often gives rise to intermetallic compounds whose subsequent oxidative dissolution differs from those recorded for the individual metals

separately [84]. In spite of these drawbacks, anodic stripping peaks can be used for a very sensitive metal detection because their height can be increased by following an analytical strategy well-known in conventional stripping analysis [84]. This consists of the application of a constant potential sufficiently negative to ensure the reduction of the starting compound to the corresponding metal. This electrodeposition (or electrogeneration) step increases the amount of the deposited metal and, consequently, enhances the peak current of the oxidative dissolution process when the potential is again scanned in the positive direction.

The usefulness of this kind of analysis is illustrated in Fig. 2.11 where the square wave voltammograms for azurite, smalt, and two samples from the frescoes painted by Palomino (1707) in the Sant Joan del Mercat church in Valencia (Spain) are shown. Copper pigments yield a unique stripping peak at -0.05 V, whereas cobalt pigments produce a main anodic peak at $+0.02$ V, accompanied by overlapping

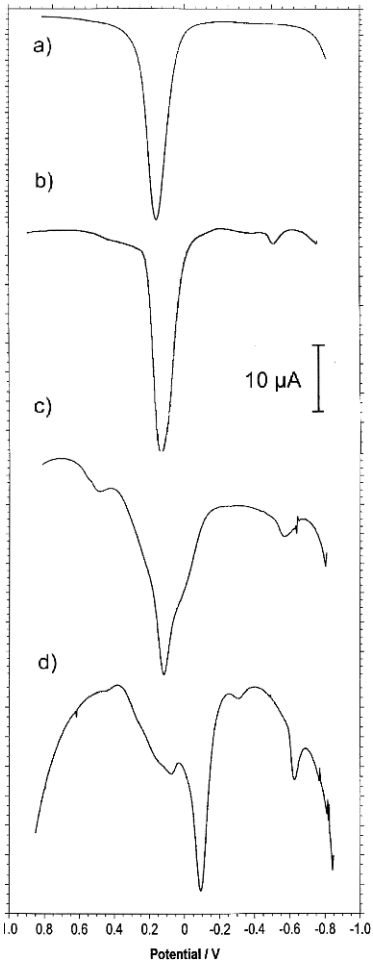

Fig. 2.11 Square wave voltammograms for blanks of azurite and smalt, and for two samples from the Palomino's frescoes in the *Sant Joan del Mercat* church in Valencia, in contact with 0.50 M potassium phosphate buffer, pH 7.4: (**a**) azurite, (**b**) sample PV8b, (**c**) smalt, and (**d**) sample PA5b. Potential scan initiated at -0.85 mV in the positive direction. Potential step increment 4 mV; square wave amplitude 15 mV; frequency 2 Hz [133]

peaks at −0.02 and +0.22 V. One of the samples yields only the stripping peak for copper, while the other exhibits a more complicated profile that can be described as the result of the superposition of stripping peaks for copper and cobalt. Interestingly, in this voltammogram, an additional stripping peak appears at −0.48 V, due to the presence of Naples yellow in the sample [126, 133]. Similar considerations can be applied for elucidating the presence of cinnabar and minium in pictorial samples [111]. It is known that cinnabar, a relatively expensive pigment, was frequently used by the artists in "noble" red portions of their paints, replacing it by minium and minium/cinnabar mixtures in other portions. Electrochemical data provide easy and sensitive proof of this practice during the Middle Age.

2.5 Identification of Metallic Species

Identification of metal particles dispersed in pictorial or decorative layers in works of art is often difficult for microscopy techniques because of: (i) their presence as highly diluted components and concentrated in microparticles that, in turn, are included in binding media and attached to priming and protective layers; (ii) the coexistence of metals with priming, ground or pigmenting layers in the samples; and (iii) the presence of products resulting from the alteration of metals.

It is therefore frequently difficult to find punctual areas in the sample having a sufficient concentration of the desired analyte to be detected by the x-ray microanalysis system. Thus, identification and eventually quantitation of metals in decorative/protective layers of pictorial samples by SEM/EDX frequently require an accurate and often time-consuming scanning process.

Metal particles display highly sensitive oxidative dissolution processes resulting in very typical stripping peaks in voltammograms. This is illustrated in Fig. 2.12, where the square wave voltammetric response of a gold-containing sample from the vault *Sant Joan del Mercat* church in Valencia (Spain) is depicted. This frescoe was painted by Acisclo Palomino in 1707 and suffered considerable damage from gunfire during the Spanish civil war in 1936. As a result, strongly deteriorated paint layers survived where the presence of gold microparticles was not clearly detected by SEM/EDX because of the large dilution of such particles in the pictorial layer. Using acetate buffer plus NaCl, the voltammogram exhibits gold-characteristic anodic peaks near to −0.2 and +1.1 V, preceded by the stripping of lead at −0.48 V due to the presence of lead pigments (Naples yellow and lead white). A similar situation was described of gold traces in the *Sant Giovanni* church in Taormina (Italy) [134]. The oxidation processes at the more positive potential can, in principle, be represented as [135, 136]

$$2Au_s + 3H_2O \rightarrow Au_2O_{3s} + 6H^+_{aq} + 6e^- \tag{2.9}$$

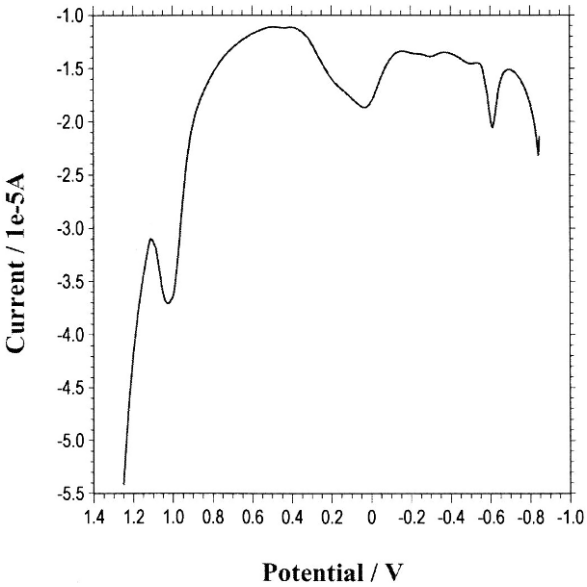

Fig. 2.12 Square wave voltammogram for a sample from the ceiling vault of the *Sant Joan del Mercat* church in Valencia (Spain), painted by Aciclo Palomino in 1707. Electrolyte: 0.50 M HAc + 0.50 M NaAc aqueous buffer plus 0.05 M NaCl (pH 4.85). Potential scan initiated at −850 mV in the positive direction. Potential step increment 4 mV; square wave amplitude 25 mV; frequency 5 Hz

while overlapping processes at less positive potentials may be attributed to the formation of gold-chloride complexes in the solution phase [134]:

$$Au_s + 4Cl^-_{aq} \rightarrow AuCl^-_{4\ aq} + 3e^- \tag{2.10}$$

2.6 Identification of Species Using Reductive/Oxidative Dissolution Process

A number of electrochemical processes involving solid materials can be described in terms of the reductive or oxidative dissolution of such materials. Within this type of processes, one can include the stripping of metal deposits previously mentioned. In the context of archaeometry, conservation, and restoration sciences, the reductive dissolution of iron oxide-type materials is of particular interest. Thus, application of the voltammetry of the microparticles approach for identifying iron pigments has been described [108, 137–139].

A typical example of these processes is shown in Fig. 2.13, where the cyclic voltammetry of (a) hematite, and (b) goethite-modified PIGEs immersed into 0.10 M HCl are depicted. As can be seen in this figure, a prominent cathodic peak is

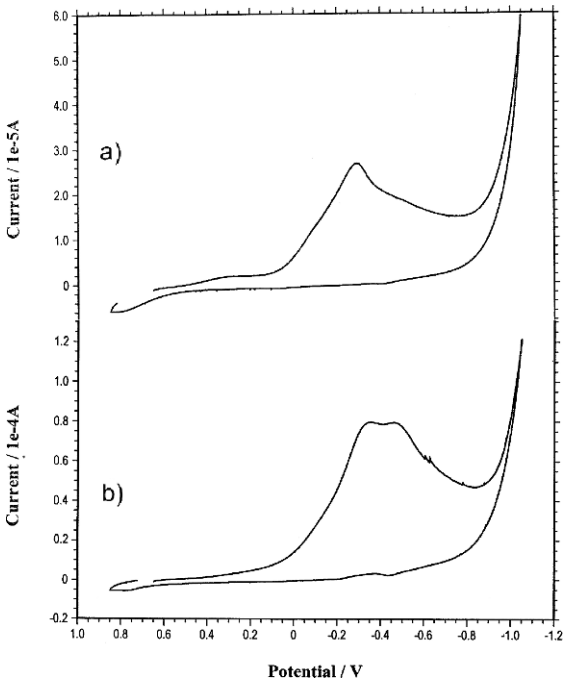

Fig. 2.13 CVs of of PIGEs modified with: (**a**) hematite, (**b**) goethite immersed into 0.10 M HCl. Potential scan rate 50 mV/s [138]

recorded at −0.45 V, with no coupled anodic signals. Interestingly, the voltammetric peaks exhibit a sharp current decay after the peak, clearly differing from the smooth decays typically observed in solution-phase electrochemistry (see Fig. 2.2). The shape of voltammetric curves depends on the mineralogical composition, but also on the shape and size distribution, of particles. Then, voltammograms of different pigments provide remarkably different profiles, as shown in Fig. 2.14. Here, square wave voltammograms for (a) *Caput mortum*, and (b) Venetian red attached to PIGEs in contact with 0.10 M HCl are depicted. The electrochemistry of iron oxides and related minerals has attracted considerable attention [137–148]. Following Grygar [144–148], this voltammetry can be described in terms of the reductive dissolution of solid Fe_2O_3 (hematite) and FeO(OH) (Goethite) to Fe^{2+} ions in solution:

$$Fe_2O_{3s} + 6H^+_{aq} + 2e^- \rightarrow 2Fe^{2+}_{aq} + 3H_2O \tag{2.11}$$

$$FeO(OH)_s + 3H^+_{aq} + e^- \rightarrow Fe^{2+}_{aq} + 2H_2O \tag{2.12}$$

Oxidative dissolution processes can also be used for identifying solid materials. This is the case of chromium (III) oxide—a green pigment that produces a well-defined anodic signal in acidic electrolytes near to +1.0 V, as can be seen in Fig. 2.15. This corresponds to the electrochemical process [147, 149]:

$$Cr_2O_{3s} + 4H_2O \rightarrow {Cr_2O_7}^{2-}{}_{aq} + 8{H^+}_{aq} + 6e^- \tag{2.13}$$

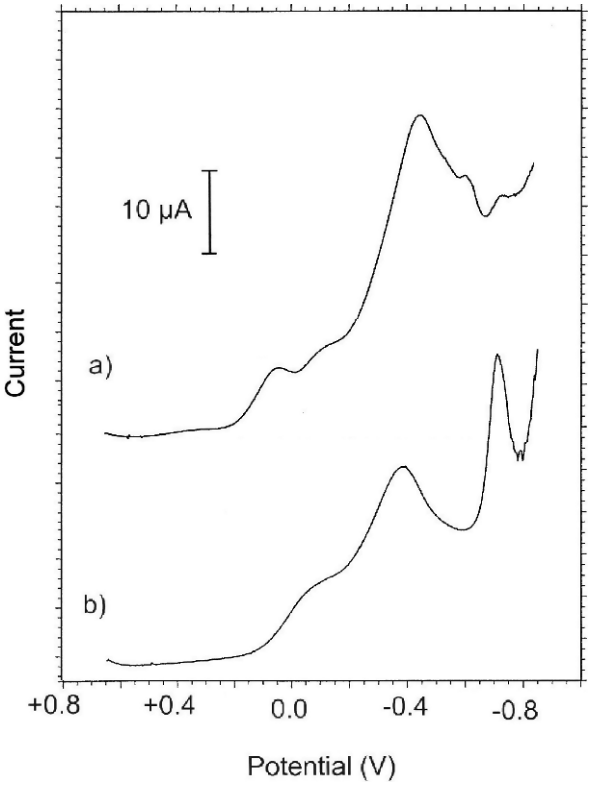

Fig. 2.14 SQWVs of PIGEs modified with: (**a**) *Caput mortum*, (**b**) Venetian *red*, immersed into 0.10 M HCl. Potential scan initiated at +0.65 V in the negative direction; potential step increment 4 mV; square wave amplitude 25 mV; frequency 5 Hz [139]

2.7 Identification of Species Via Solid-State Transformations

The electrochemical processes involving Prussian blue and organic dyes studied above can be taken as examples of solid state redox processes involving transformation of a one solid compound into another one. This kind of electrochemical reactions are able to be used for discerning between closely related organic dyes. As previously described, the electrochemistry of solids that are in contact with aqueous electrolytes involves proton exchange between the solid and the electrolyte, so that the electrochemical reaction must in principle be confined to a narrow layer in the external surface of the solid particles. Eventually, however, partial oxidative or reductive dissolution processes can produce other species in solution able to react with the dye.

The characterization of individual dyes is complicated by: (a) the existence of a significant structural similarity, and consequently, reactivity, for different dyes; (b) several dyes are composed of mixtures of pigmenting compounds, in turn having

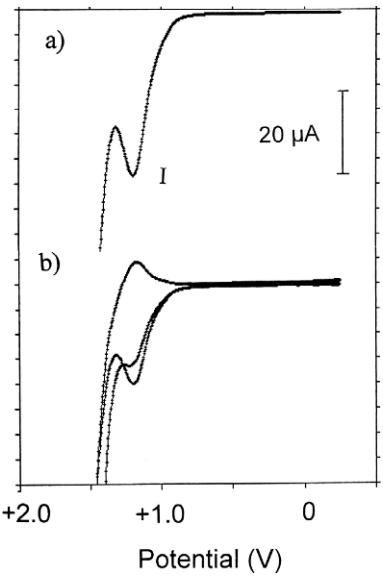

Fig. 2.15 SQWV for Cr_2O_3 immersed into 0.10 M HCl shown: (**a**) the net difference current between forward and backward pulses, and, (**b**) such currents and their sum. Potential scan initiated at +0.15 V in the positive direction. Potential step increment 4 mV; square wave amplitude 25 mV; frequency 5 Hz. Adapted from [149]

a close structural similarity. Scheme 2.1 shows structure diagrams for typical anthraquinonic and flavonoid compounds.

Figure 2.16 compares the SQWV responses obtained for silk fibbers pigmented with: (a) *granado*; (b) *alazor*; (c) curcuma, (d) weld, and (e) cochineal red in contact with acetic/acetate buffer. This voltammetry yields clearly different responses for the involved dyes, thus allowing for an electrochemical identification of pigments in samples.

The electrochemistry of anthraquinonic compounds in solution is dominated by the proton-assisted reduction of the quinone group to diphenol. Flavonoid and anthraquinonic compounds undergo electrochemical oxidations through [150–154] the orthophenol moiety, while their reduction can occur through the keto group of the benzopyrone moiety yielding hydroxyl derivatives at potentials ca. −1 V [150–154]. It should be noted, however, that the presence of additional phenol groups can complicate the electrochemical response of flavonoids. Thus, Brett and Ghica have recently reported [155] that the electrochemical oxidation of quercetin (3,3′,4′,5,7-pentahydroxyflavone) on glassy carbon electrodes occur in a cascade mechanism, related to the two catechol hydroxy groups and the other three hydroxyl groups that are all electroactive. Adsorption complicates the voltammetric response, and the final oxidation product is not electroactive and blocks the electrode surface [155]. Chalcones, further oxidized to flavonoids at potentials above +0.5 V [156–158], can also be involved.

These electrochemical processes can be accompanied by secondary reactions in solution. The presence of additional phenol groups can complicate the electrochemical response of flavonoids, giving rise to additional electrochemical processes [150–158]. This fact is of interest for analytical purposes, because

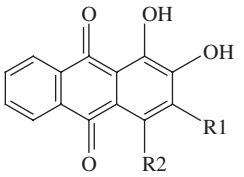

alizarin R1 = H, R2 = H
purpurin R1 = H, R2 = OH
pseudopurpurin R1 = COOH, R2 = OH

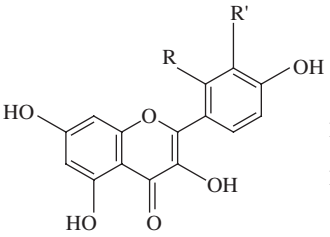

R = H, R' = OH: Luteolin

R = OH, R' = H: Morin

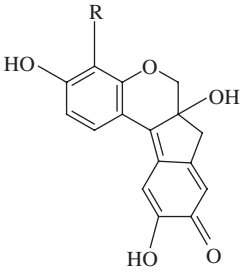

R = H: Brazilein

R = OH: Haematein

Scheme 2.1 Structural representations of typical anthraquinonic, flavonoid, and flavonoid-related dyes

additional dye-characteristic voltammetric peaks can appear. As a result, the solution phase electrochemistry of organic dyes is strongly dependent on the electrolyte composition and electrochemical conditions.

The voltammetric response of curcumin and carthamin must, in principle, be dominated by the oxidation of the phenol and/or methoxyphenol groups (see Scheme 2.2). The electrochemistry of methoxyphenols has claimed considerable attention because of their applications in organic synthesis [159–163]. As studied by Quideau et al., in aprotic media, 2-methoxyphenols are oxidized in two successive steps into cyclohexadienone derivatives [163], whereas α-(2)- and α-(4-methoxyphenoxy) alkanoic acids undergo electrochemically induced spirolactonization to develop synthetically useful orthoquinone bis- and monoketals. In the presence of methanol, the electrochemical pathway involves an initial one-electron loss, followed by proton loss, to form a monoketal radical. This undergoes a subsequent electron and proton loss coupled with the addition of alcohol to form an orthoquinone monoketal. The formal electrode potential for the second electron transfer

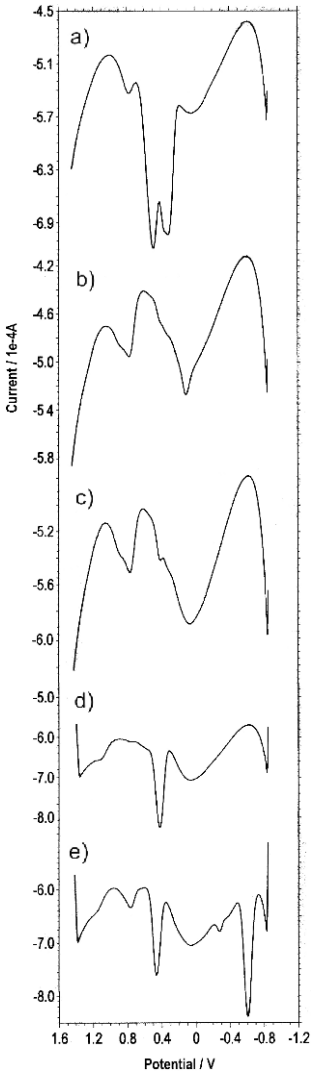

Fig. 2.16 SQWVs for silk fibers pigmented with: (**a**) *granado*; (**b**) *alazor*; (**c**) curcuma, (**d**) weld, and (**e**) cochineal *red* in contact with acetic/acetate buffer (total concentration 0.50 M) at pH 4.85. Potential step increment 4 mV; square wave amplitude 25 mV; frequency 5 Hz

is lower than that of the first electron transfer, thus resulting in an apparently unique irreversible oxidation voltammetric signal. In aqueous media, p-methoxyphenols yield p-benzoquinone.

Examples of the application of solid state electrochemistry to identifying dyes in textile samples can be provided. Thus, Fig. 2.17 compares the square wave voltammograms of: (a) saffron blank, and (b) sample from a Tibet temple, attached to fluorine-doped tin oxide (FTO) electrodes immersed into acetate buffer. After initiating the potential scan at −0.85 V in the positive direction, two separated oxidation

Scheme 2.2 Structural diagrams for curcumoid compounds curcumin and carthamin

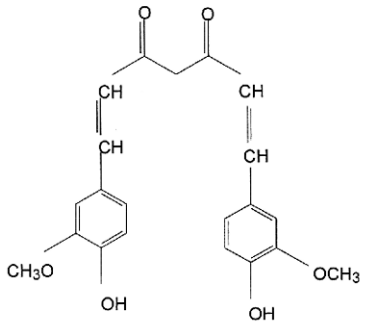

Curcumin

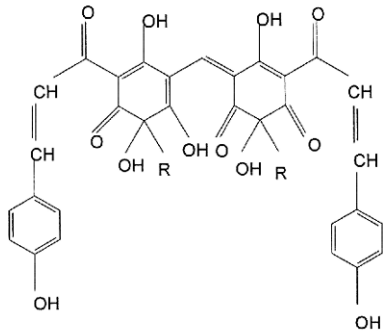

Carthamin

peaks at −660 and −140 mV were recorded. A close similarity was obtained between the reference saffron and the studied sample.

Application of this methodology to the analysis of materials in textiles can be illustrated by the identification of pigmenting species in brocade pieces from the church of Castellfort (Valencian Region, Spain), dated from the 25th century (see Fig. 2.18) [124]. Here, microsamples from fibers were transferred to the surface of paraffin-impregnated graphite electrodes. The voltammetric response, in contact with acetate buffer for a sample from a scapulary, is compared in Fig. 2.19 with those of carmine and Brazilwood. Examination of such voltammograms clearly suggests that the sample contains a mixture of the above dyes as pigmenting materials.

2.8 Analytical Strategies

The analytical capabilities of solid state electrochemical techniques can be increased by "chemical" and "electrochemical" procedures. By the first means, the most direct approach consists in the sequential use of different electrolytes incorporating

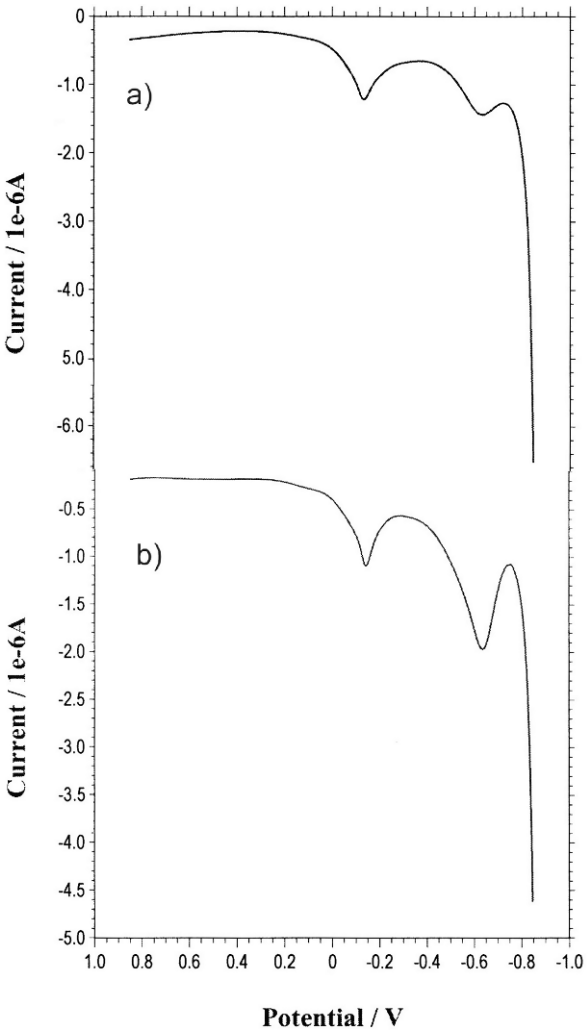

Fig. 2.17 SQWVs of FTO electrodes modified with: (**a**) *saffron*, and, (**b**) sample from Tibet temple immersed into 0.50 M acetic acid +0.50 M sodium acetate aqueous buffer at pH 4.85. Potential scan initiated at −0.85 V in the positive direction; potential step increment 4 mV; square wave amplitude 25 mV; frequency 2 Hz. Courtesy of the Philadelphia Museum of Arts

species able to react with some functional groups of the analytes. The basic idea is that in the presence of a specific reagent, the voltammetric response of each component must change with respect to that previously obtained in the absence of the reagent. By the second means, different electrochemical parameters can be varied in order to improve the electrochemical recognition of selected compounds—namely, initial and switching potentials and the potential scan rate in cyclic voltammetry, and the initial and final potentials, as well as potential step increment, square wave amplitude, and frequency in square wave voltammetry. Additionally, application of

Fig. 2.18 Image of a scapulary from the mediaval textile workshops in Morella (Valencian Region, Spain) existing in the church of Castellfort (Valencian Region, Spain), dated from the 25th century

polarization steps (repeatedly cycling the potential between two given values or applying a constant potential during a given "electrogeneration time" can result in significant differences between the pre- and post-treatment voltammetric record). Thus, the voltammetric response of anthraquinonic and flavonoid compounds is particularly sensitive to the application of negative polarization potentials—a feature previously noted [122] and also observed by Grygar et al. [123] and Dai and Shin [164] for anthraquinone-type compounds.

The first strategy can be illustrated by the effect of the addition of boric acid (H_3BO_3) or $AlCl_3$ to acetate buffers with respect to the response of flavonoid dyes [124]. We know that boric acid coordinates with compounds containing o-diphenol groups, which form stable adducts in solution [165]. In turn, Al^{3+} ions form strong complexes with flavonoids containing 3- and 5-hydroxy groups [166]. Assuming that solid compounds can also form surface-confined adducts with those coordinating agents, one can expect that the response of solid dyes containing o-diphenol and/or 3- and 5-hydroxy groups should change in the presence of the above species.

Experimental data for flavonoid dyes confirmed these expectances [124]. Thus, the voltammetric response was expected—the square wave voltammograms of flavonoids containing 3- and 5-hydroxy groups change from 0.25 M HAc + 0.25 M NaAc to that plus 0.05 M $AlCl_3$. The obtained results are illustrated in Fig. 2.20. First, the SQWVs of weld-modified PIGEs in the absence (Fig. 2.20a) and presence (Fig. 2.20b) of Al^{3+} are shown. Coordination with aluminium apparently blocks electron-transfer processes, and the peaks are significantly decreased. For logwood, the contrast between the square wave voltammograms in the absence and presence

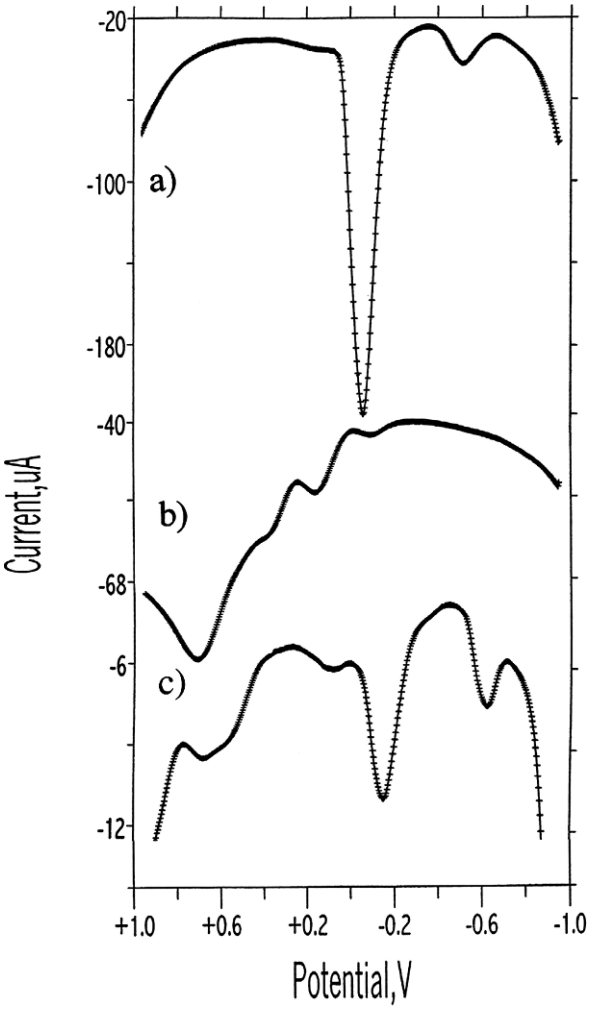

Fig. 2.19 Square wave voltammograms for: (**a**) carmine, (**b**) Brazilwood, and (**c**) a fiber sample from a mediaeval scapulary found in the church of Castellfort (Valencian Region, Spain). Electrolyte: 0.50 M sodium acetate buffer. Potential step increment 4 mV; square wave amplitude 25 mV; frequency 5 Hz. Adapted from [124]

of Al^{3+} (illustrated in Fig. 2.20c and d) is also remarkable. In this case, voltammetric peaks are all decreased except the peak at +0.03 V, which is abruptly enhanced. This probably results from the formation of an adsorbate of the aluminum complex on the electrode surface—a situation similar to that existing in alizarin-type aluminium complexes [124]. A similar situation occurs when boric acid is added to the electrolyte with regard to dyes containing o-phenol moieties, due to the strong complexation of such groups by borate units. Structural diagrams for the aforementioned coordination are depicted in Scheme 2.3.

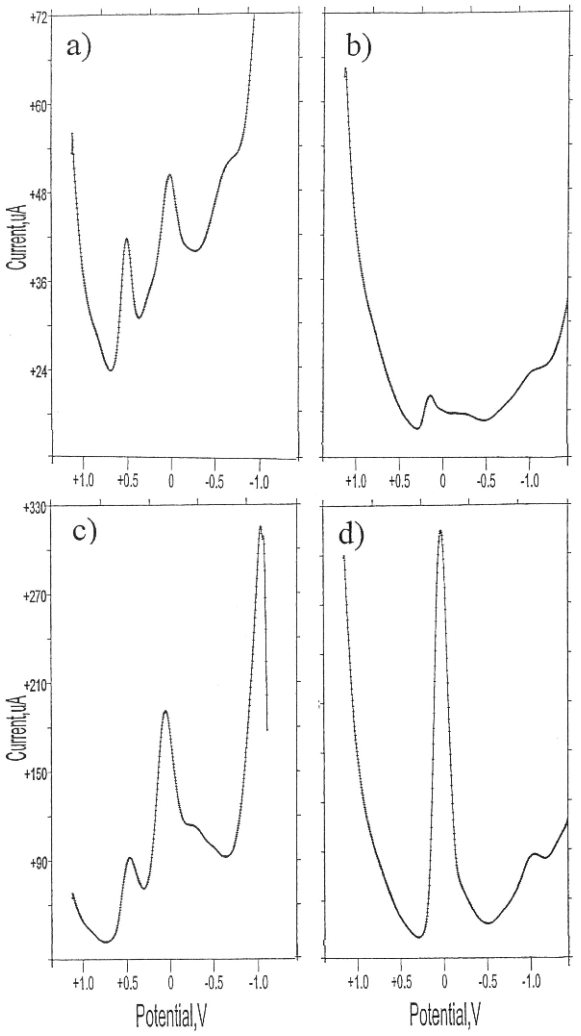

Fig. 2.20 SQWVs (first scan) of weld (**a**, **b**) and logwood (**c**, **d**) immersed into 0.25 M HAc + 0.25 M NaAc (**a**, **c**) and that electrolyte plus 0.05 M $AlCl_3$ (**b**, **d**). Potential step increment 4 mV; square wave amplitude 25 mV; frequency 15 Hz [124]

The described procedures are able to distinguish organic dyes in solid samples. However, in several cases the distinction between some pigments can be made uncertain by matrix effects. These can be attributed mainly to (a) the presence of additional peaks associated with other dyes and/or priming and protective organic compounds coexisting in the sample; (b) occurrence of cross reactions between the intermediate products of electron-transfer processes; (c) modification of the electrochemical response of the dyes as an effect of complexation reactions with metal ions from inorganic pigments; or (d) appearance of unexpected peaks associated with alteration products.

The application of constant potential steps results in the generation of new solid compounds whose electrochemical response should differ from the original

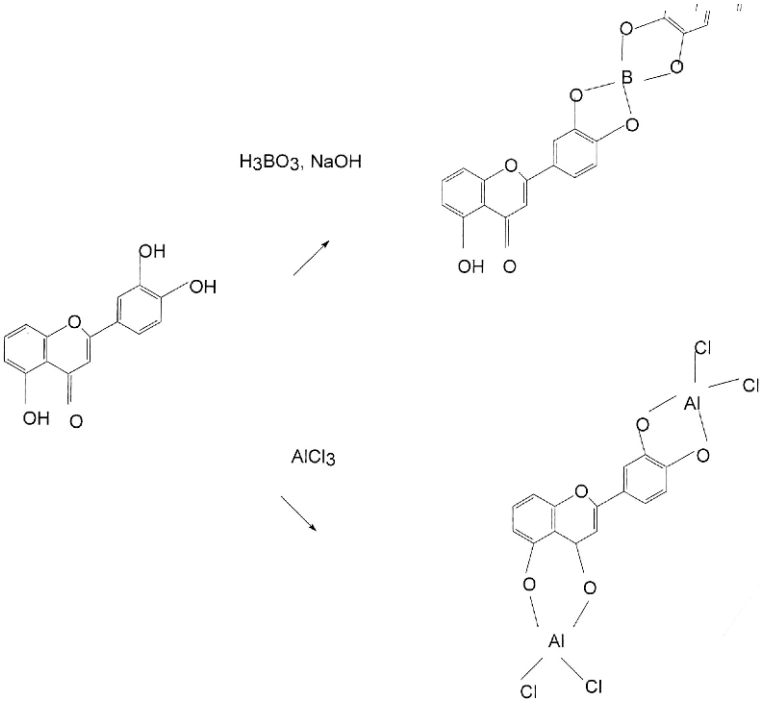

Scheme 2.3 Adduct formation between flavonoids and boric acid and aluminum chloride [124]

material. The use of the responses of the parent material and its electrochemically generated derivative can be used for discerning similar materials.

This strategy is illustrated in Figs. 2.21 and 2.22 for the case of alizarin. The parent dye exhibits two main peaks at +0.40 and −0.60 V, corresponding respectively to the oxidation of the o-phenol moiety and the reduction of the quinone group. After application of a reduction step at −1.50 V, the resulting polyhydroxy species produces overlapping oxidation signals at +0.5 and −0.07 V.

Oxidative treatments also yield significant changes in the voltammetric response. As shown in Fig. 2.22, the response of alizarin changes remarkably after application of an anodic step. Oxidation of alizarin should make polyquinone species able to be electrochemically reduced at potentials differing from those at which the parent alizarin reduces. As a result, the voltammetric pattern also changes drastically. Application of this strategy increases the number of parameters that can be used as diagnostic criteria for identifying dyes.

It should be noted, however, that the changes in the voltammetric response are conditioned by the nature of the extent of the redox reaction across the solid. Thus, for organic solids in contact with aqueous electrolytes, and using the aforementioned model of Lovric, Scholz, Oldham, and co-workers [115–118], the propagation of the redox reaction should involve proton hopping coupled with electron hopping between adjacent immobile molecules [119–125]. Chronoamperometric data

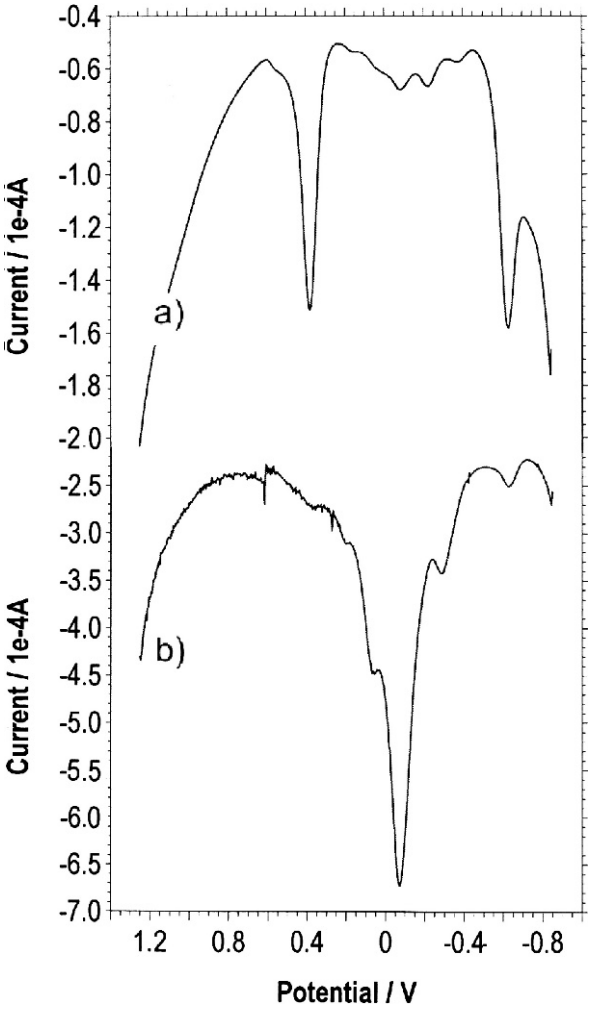

Fig. 2.21 Square wave voltammograms for alizarin-modified paraffin-impregnated graphite electrodes immersed into 0.50 M potassium phosphate buffer (pH 7.0): (**a**) before, and (**b**) after application of a potential step of −1.50 V during 15 min. Potential initiated at −0.85 V in the positive direction. Potential step increment 4 mV; square wave amplitude 25 mV; frequency 5 Hz

reveals that electron diffusion in organic compounds in contact with aqueous buffers is significantly faster than proton diffusion [167]. Accordingly, application of a reductive step could produce a situation similar to that ideally represented in Fig. 2.23. The inverse case, when electron transport was clearly faster than proton transport, is schematized in Fig. 2.24. The voltammetric response of these systems should be different to that of the parent solid.

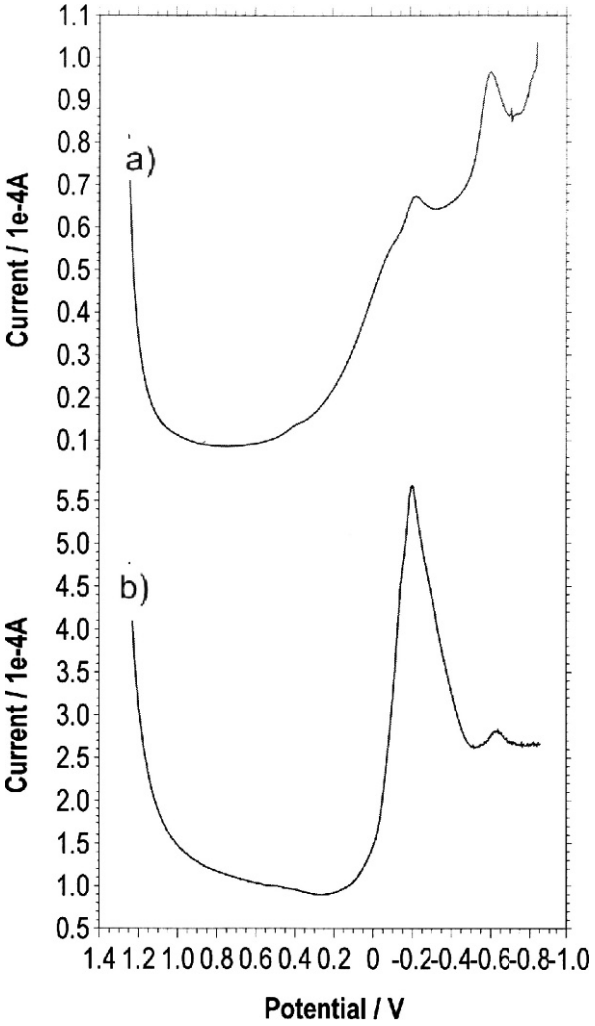

Fig. 2.22 Square wave voltammograms for alizarin-modified paraffin-impregnated graphite electrodes immersed into 0.50 M potassium phosphate buffer (pH 7.0): (**a**) before, and (**b**) after application of a potential step of +1.50 V during 15 min. Potential initiated at +1.25 V in the negative direction. Potential step increment 4 mV; square wave amplitude 25 mV; frequency 5 Hz

Topographic AFM examination of organic dyes under the application of reductive and oxidative potentials appears to be consistent with the above modeling [168]. This can be seen in Fig. 2.25 where in situ AFM images from the upper face and sides of crystals of indigo (a) before, and (b) after application of a linear potential step between 0.0 and +0.75 V at a potential scan rate of 10 mV/s are shown. Here,

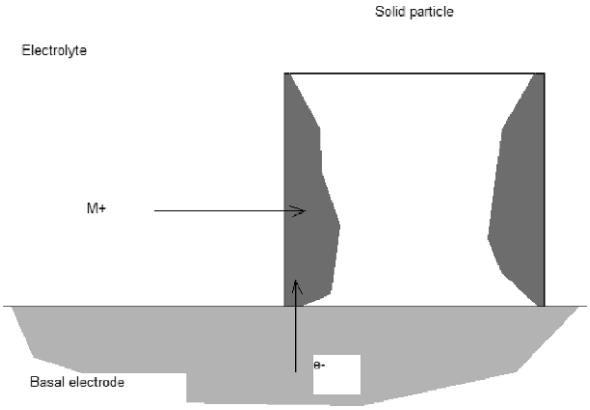

Fig. 2.23 Schematics representation of the electroactive layer in the case of the electrochemical reduction of a solid when ion diffusion through the solid is allowed—electron diffusion is highly hindered

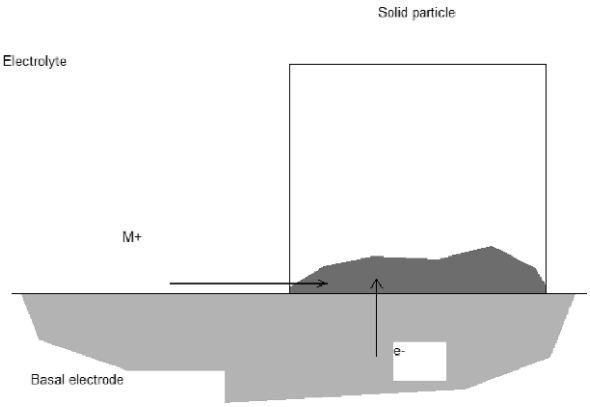

Fig. 2.24 Schematic representation of the electroactive layer in the case of the electrochemical reduction of a solid when electron diffusion through the solid is allowed and ion diffusion is highly hindered

an agglomerate of crystals of ca. $1 \times 0.5\,\mu m$ exhibits significant changes during the potential scan, consisting of apparent erosions of several regions of lateral sides, while other regions become apparently extended. A possible scheme for explaining these features may consist of an initially topotactic process, eventually accompanied by exfoliation and restacking, and followed by crystal restructuring and eventually phase transition. The maximum extent of the lateral distortions of crystals can be estimated as long as ca. 50–80 nm—a value that is in close agreement with that calculated for the breadth of the diffusion layer from chronoamperometric data, taking $D = D_H = 2 \times 10^{-10}\,cm^2/s$. [167, 168].

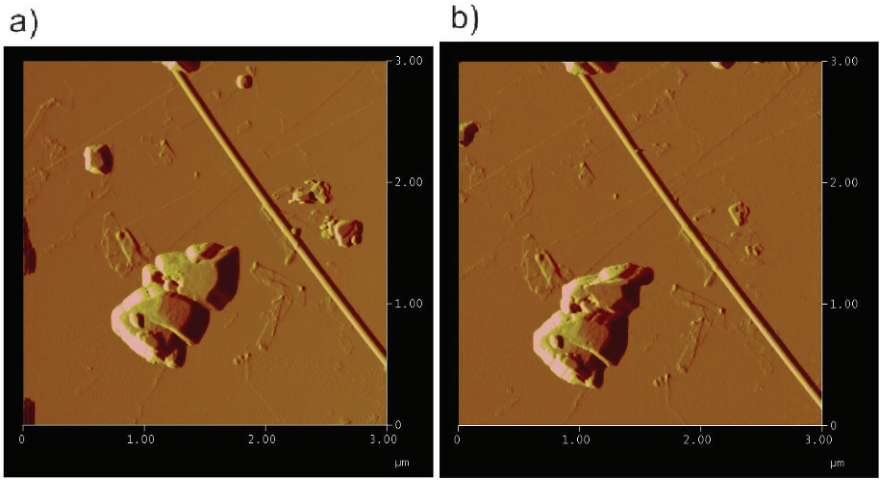

Fig. 2.25 AFM of indigo crystals adhered to a graphite plate in contact with 0.50 M sodium aqueous acetate buffer (**a**, **c**) before, and (**b**, **d**) after application of a linear potential scan between 0.00 and +0.75 V at a sweep rate of 10 mV/s [168]